

Monte Carlo Simulation of Neutral Xenon Flows in Electric Propulsion Devices

Iain D. Boyd,* Douglas B. Van Gilder,† and Xiaoming Liu‡
Cornell University, Ithaca, New York 14853-7501

Numerical simulations of neutral xenon flow in three different electric propulsion configurations are presented. Flows through an ion thruster, a plasma contactor, and a Hall thruster are considered. The computations are performed using a Monte Carlo method. The ion thruster configuration chosen for study is the UK-10 engine. Comparisons of the simulations are made with a simple analytical model that has been used in previous computations of backflow from ion thrusters. Both sets of theoretical results are compared with number density measurements. The Monte Carlo simulations provide closer agreement with the experimental data and the analytical model is found to overpredict density in the backflow plume region. The Monte Carlo simulation of the plasma contactor plume also compares well with experimental measurements. For the Hall thruster, the simulations reveal detailed structures of the fluid flow in the anode chamber. Comparison with a measured data point for velocity indicates that the experiment is compromised by a relatively high facility back pressure. Inclusion of the back pressure in the simulation leads to excellent agreement with the datum.

Introduction

XENON is the propellant of choice for many electric propulsion devices. For example, use of xenon ion thrusters is now planned on several spacecraft missions including the New Millennium program of NASA, the HS-601 and HS-702 satellites of Hughes, and the ARTEMIS spacecraft of the European Space Agency. Russian Hall thrusters using xenon have been flying for many years. This propellant is also being considered for use in resisto-jets¹ and pulsed plasma thrusters.² While increasing the use of electric propulsion in space indicates acceptance of the reliability and performance of this technology, there is a continued need for detailed analysis of these systems for two specific reasons. First, the thrust efficiencies of electric propulsion devices are low, e.g., 50% for an ion thruster. Improvement in this performance is most likely attained through a comprehensive understanding of the operation of the device. Second, there is a concern with the interaction between the spacecraft and the plume flowfield generated by the thruster. For ion thrusters, the impact of heavy metallic ions sputtered from the acceleration grids is of particular concern. These ion impacts are most problematic in the plume blackflow region behind the thruster exit plane. The ions are accelerated into this region by the electric fields associated with the charge exchange plasma. In addition, the charge exchange ions may be accelerated back toward the grids of the thruster, causing erosion.

The present study considers numerical simulation of xenon plumes from electric propulsion devices. As explained in the preceding text, the main issue in such plumes is the charge exchange phenomenon in which a high-energy ion collides with a low-energy neutral atom to produce a low-energy ion and a high-energy atom. The low-energy ion has the possibility to diffuse into the thruster backflow region, creating electric fields that may ultimately attract heavy metallic ions sputtered

from accelerating grids or from internal thruster surfaces. Any computation that aims to model these phenomena accurately must simulate both the xenon ions and the xenon atoms. The specific focus of the work presented here concentrates on the simulation of the xenon atoms. A separate study considers the effects of the ions in an ion thruster.³

In this paper, a description is first made of the computer code and physical models employed for the numerical simulations. Results of neutral xenon flow computations are then presented for three different configurations. First, flow is computed for the UK-10 ion thruster. Comparison of the simulated results is made with a simple analytical model and with experimental measurements. Next, results for a plasma contactor geometry are provided and again comparison with measured data is provided. Finally, simulation results are presented for neutral xenon flow through a Hall thruster geometry.

Numerical Method

In plumes from many electric propulsion devices, both collision and plasma effects are important. A computer code has been developed that simulates these phenomena using a combination of two different particle methods. The collisions are treated using the direct simulation Monte Carlo method (DSMC).⁴ In this technique, particles move through physical space undergoing collisions with other particles and with solid surfaces. A computational grid is employed to group together particles that are likely to collide, and for evaluating macroscopic flow properties. A novel implementation of the DSMC technique has been developed⁵ for efficient numerical performance on a range of computer platforms. The code may be executed on scalar workstations and parallel supercomputers. The DSMC code is called MONACO,⁵ and has been successfully applied to low-density problems in spacecraft propulsion, hypersonics, and plasma processing of materials. Plasma effects are treated using the particle in cell method (PIC).⁶ This method uses particles to weight the charge density to the nodes of the computational grid. The charge density defines the potential and, hence, the electrostatic field forces that affect the trajectories of the charged particles. Details of the implementation of this hybrid computer code are provided in Ref. 3.

In the studies described here, only the DSMC portion (MONACO) is employed to simulate a number of different neutral xenon flows. The motivation for studying the neutral

Received Oct. 9, 1997; revision received May 10, 1998; accepted for publication May 25, 1998. Copyright © 1998 by the American Institute of Aeronautics and Astronautics, Inc. All rights reserved.

*Associate Professor, Sibley School of Mechanical and Aerospace Engineering. Senior Member AIAA.

†Research Assistant, Sibley School of Mechanical and Aerospace Engineering.

flow only is to demonstrate the accuracy of the DSMC-PIC code for simulating the behavior of the atoms in the absence of plasma effects. The importance of accurate computation of the neutral flowfield should not be underestimated because it participates directly in the creation of any charge exchange plasma. One of the strengths of MONACO lies in its use of unstructured grids that provides great flexibility in terms of simulating geometric complexity. In all simulations performed here, the variable hard sphere (VHS) collision model of Bird⁴ is employed. For neutral xenon, the model parameters are reference collision diameter, $d_{ref} = 5.74 \times 10^{-10}$ m, and viscosity temperature exponent, $\omega = 0.62$.

Results

The flow of xenon atoms is computed for three different electric propulsion configurations. Specifically, these are 1) the UK-10 ion thruster, 2) a plasma contactor, and 3) a Hall thruster. In each of the investigations described next, the cell sizes are scaled locally to be less than one mean free path. Sensitivity studies to cell size and time-step were undertaken to ensure independence of the numerical results to these computational parameters.

Ion Thruster

The specific reason for considering the UK-10 thruster is the availability of experimental measurements by Crofton⁷ of the flow of neutral xenon atoms through the device with the current turned off. The simulations begin at the thruster exit plane using input conditions of a flow rate of 0.61 mg/s, a Mach number of 1, and a stagnation temperature of 295 K. The plume is assumed to expand into a vacuum. An important issue in simulating the UK-10 thruster concerns the interaction between the neutral flow and the dish grids employed in this device. In the results presented here, it is assumed that the grids have no effect on the neutral flow and that the xenon atoms exit the thruster with a mean radial velocity component of zero. A second issue concerns the distribution of the atoms across the thruster exit plane. In the results shown here, a uniform density profile is employed. The calculations using MONACO employ 11,000 cells and 100,000 particles. The flow domain extends 1 m along the axis from the thruster exit and 1 m radially. The simulation is performed on an IBM workstation and requires 6 h execution time.

In previous PIC simulations of ion thruster plumes,⁸ the neutral xenon atoms were not treated directly in the computation. Instead, the number density of atoms was approximated using the following analytical expression obtained from kinetic theory (e.g., see Ref. 4, p. 153):

$$n(R, \theta) = n_0 \{1 - [1 + (r_T/R)^2]^{-1/2}\} \cos(\theta) \quad (1)$$

where r and z are the radial and axial distances from the point on the centerline at the thruster exit, respectively; r_T is the thruster exit radius, $R = [r^2 + (z + r_T)^2]^{1/2}$, $\theta = \tan^{-1}[r/(z + r_T)]$; a is a correction factor; and n_0 is the number density at the thruster exit. This expression was used to compute a source term of charge exchange ions that led to plume backflow. One of the goals of the present study is to assess the usefulness of this expression for the UK-10 thruster.

In Fig. 1, contours of number density for the flow computed using the Monte Carlo code (upper half) and with Eq. (1) (lower half) are compared. Qualitatively, both solutions exhibit the expected behavior for a low-density plume expansion. There is a very good agreement between the two sets of results far along the axis, where the density decays with the inverse square of distance from the thruster exit. However, close to the thruster exit at large radial distances there are significant differences.

Comparison of the Monte Carlo and analytical results for number density with the experimental data of Crofton⁷ along

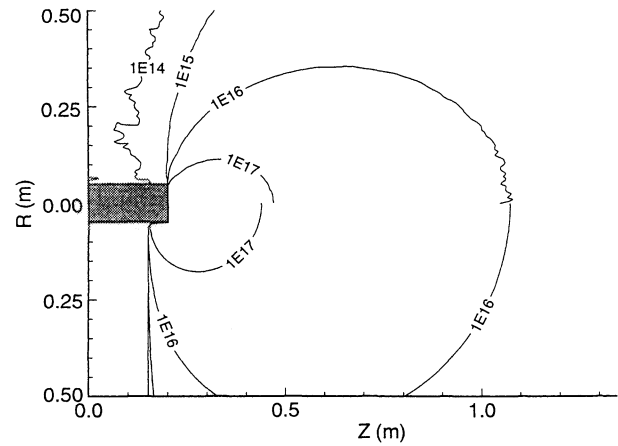


Fig. 1 Contours of number density in m^{-3} for the plume of the UK-10 ion thruster: Monte Carlo (upper) and analytical model (lower).

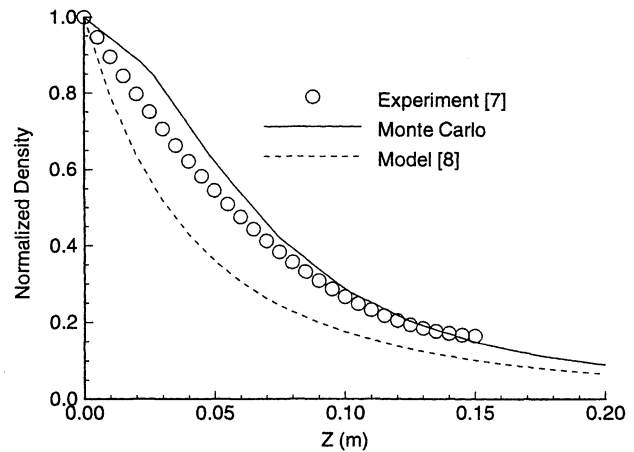


Fig. 2 Variation in normalized xenon density along the thruster plume axis.

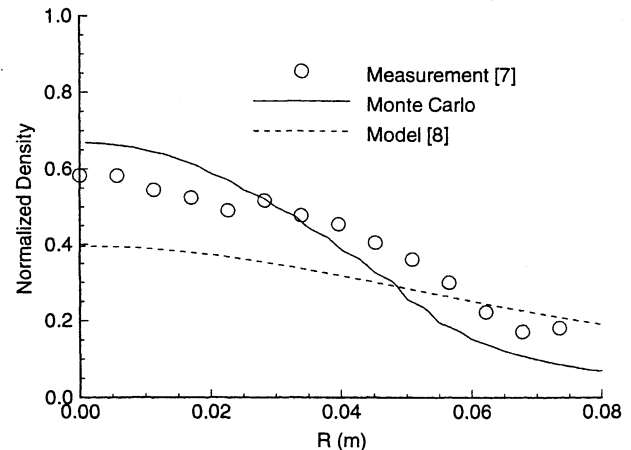


Fig. 3 Radial variation in normalized xenon density at a distance of 4.5 cm from the thruster exit plane.

the plume axis and radially at distances of 4.5 and 15 cm from the exit plane are shown in Figs. 2, 3, and 4, respectively. The experimental data were obtained using a nonintrusive, two-photon, laser-induced fluorescence technique that presents calibration difficulties. Therefore, the comparisons can only be made for normalized data. For each of the three data sets (experiment, Monte Carlo, and analytical model) the data are normalized using the value at the thruster exit plane on the plume axis. All of the experimental data shown here have been cor-

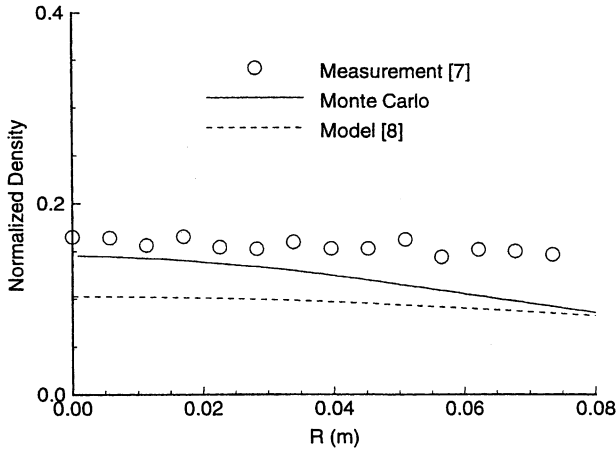


Fig. 4 Radial variation in normalized xenon density at a distance of 15 cm from the thruster exit plane.

rected for the facility effects of the vacuum chamber⁷ by adding a constant associated with the back pressure.

A good agreement between Monte Carlo prediction and measurement is obtained along the plume axis as shown in Fig. 2. The simple model, however, shows a significant underprediction of density close to the thruster exit. At large distances from the thruster, the analytical model appears to be approaching the Monte Carlo results. In the radial profile at 4.5 cm from the thruster, shown in Fig. 3, a good agreement is again obtained between the Monte Carlo simulation and the experimental data. As expected from Fig. 2, the simple model underpredicts the density on the axis by about 50% in comparison with the measured data. In addition, the model predicts a flatter profile for the plume shape. At 15 cm from the thruster, as shown in Fig. 4, all three profiles are very flat. The Monte Carlo computations continue to provide a good agreement with the experimental data. The analytical model shows an error of about 50%.

To consider in detail the importance of neutral xenon modeling for simulation of the charge exchange plasma, the ratio of the two solutions [Monte Carlo divided by Eq. (1)] is shown in Fig. 5. Note that when current is applied to the thruster, the main ion beam of the plume is confined to a cylinder of radius 5 cm about the plume axis. The contours in Fig. 5 indicate that there is, at worst, only a 50% disagreement between the Monte Carlo and model results inside this region. However, close to the thruster exit plane, just outside the main beam area, there are orders of magnitude differences between the two solutions. In particular, the analytical model overpredicts the neutral number density in this region.

It is appropriate to assess the effect on the predicted charge exchange plasma that may occur as a result of using the simple analytical model. The volumetric production rate of charge exchange ions may be written

$$v_{CEX} = n_i V_i \sigma_{CEX}(V_i) \quad (2)$$

where n_i is the ion number density, V_i is the ion velocity (much greater than neutral xenon velocity), and σ_{CEX} is the charge exchange cross section that is a function of ion velocity. Assuming that the ion density, the ion velocity, and the charge exchange cross section are all unaffected to the first order by the treatment of the neutral atoms, Eq. (2) indicates that the volumetric production depends only on the value of the neutral atom number density. The ratio of charge exchange production predicted using the Monte Carlo and analytical results for xenon density are shown in Fig. 6 along the plume axis, and in Fig. 7 along a radial line at an axial distance of 2.5 cm from the thruster exit. As seen in Fig. 6, the largest difference incurred through use of the analytical model along the plume

axis is about 65%. Because this is the region of greatest charge exchange ion production, this represents a useful estimate of the error associated with use of Eq. (1) to describe the neutral xenon atoms. In Fig. 7, it is shown that more significant differences occur at large radial distances in the region close to the thruster. Beyond the edge of the thruster exit, at 5 cm, there is significant overprediction of charge exchange ion production by the analytical model. However, as discussed earlier, the magnitude of charge exchange ion production in this region

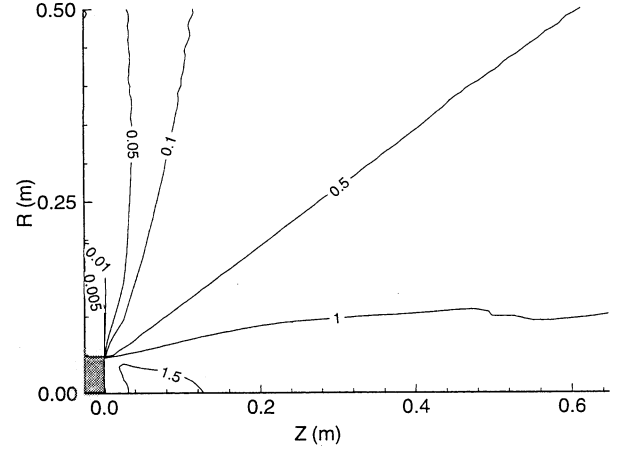


Fig. 5 Ratio of number densities: Monte Carlo prediction divided by analytical model.

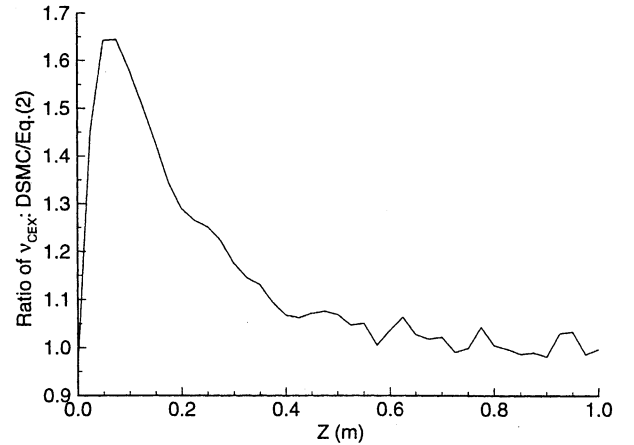


Fig. 6 Ratio of charge exchange volumetric production rates along the plume axis.

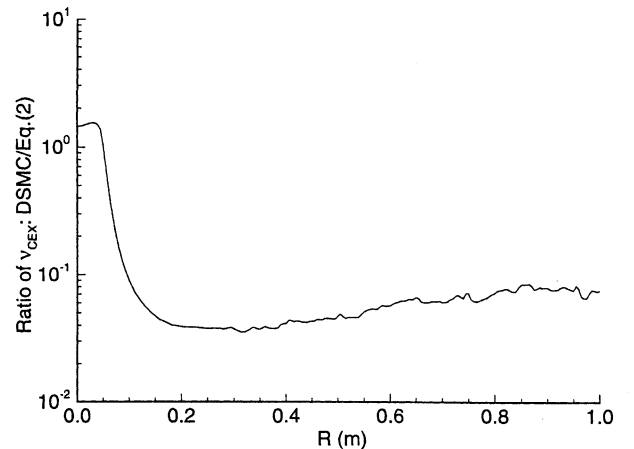


Fig. 7 Ratio of charge exchange volumetric production rates along the radial line located 2.5 cm from the thruster exit.

is significantly smaller than that in the main beam, and so the differences indicated in Fig. 7 are less important.

Plasma Contactor

Neutral xenon measurements in the plume of flow through a plasma contactor configuration were reported by Williams and Wilbur.⁹ The present computation of this flow is begun at the exit plane of the cathode. A portion of the grid used for the Monte Carlo computations is shown in Fig. 8, indicating the positions of the cathode and anode. The cathode has an exit diameter of 0.76 mm and is assumed to be at a temperature of 1300 K. Neutral xenon exits this orifice at a flow rate of 0.4 mg/s, with sonic conditions assumed. The anode is located 2 mm downstream of the cathode exit and has a total diameter of 120 mm and an orifice diameter of 5 mm. The anode temperature is assumed to be 300 K. The cathode and anode are coaxial. A back pressure of 3.1×10^{-6} torr (corresponding to a number density of 10^{17} m^{-3} at 300 K) is assumed for the vacuum chamber. The entire computational domain is shown in Fig. 9. Clustering of cells is achieved in regions of high density through a combination of triangular and quadrilateral cells.

Contours of number density in m^{-3} for the entire flowfield are shown in Fig. 10. Again, the expected trend for an orifice expansion is observed. Note in the far field that the number densities approach the vacuum chamber background level. In Fig. 11, contours of translational temperature in degrees Kelvin are shown. Here, the influence on the expansion of the anode

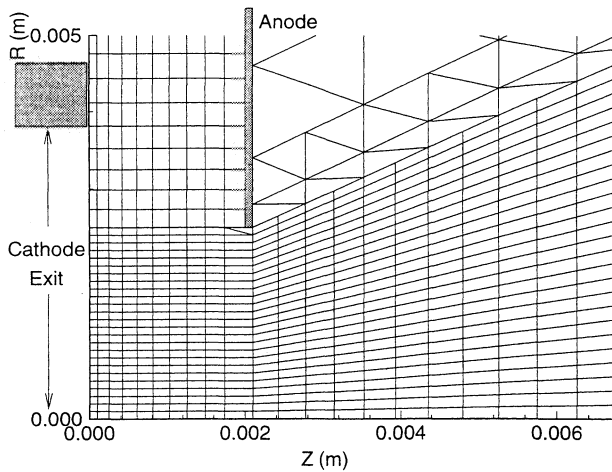


Fig. 8 Close-up view of computational grid showing geometry of cathode and anode for plasma contactor.

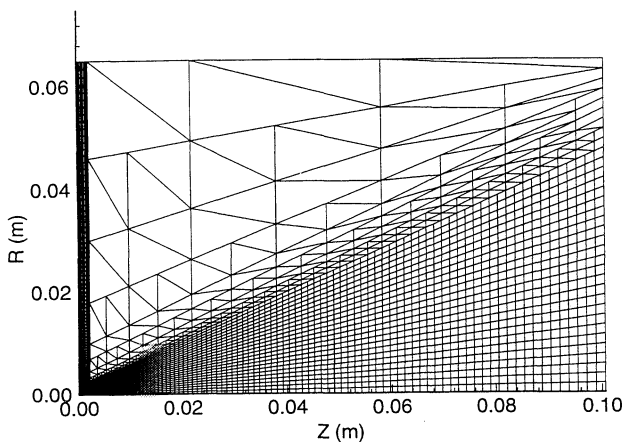


Fig. 9 Grid employed for Monte Carlo computation of plasma contactor plume illustrating mixture of quadrilateral and triangular cells.

and the finite back pressure may be seen. Close to the anode, the flow is heated to 300 K. Moving away from the orifice, the expanding flow first shows decreasing temperature. However, as the particles of the background gas interact with the expanding plume, the temperature is again raised. Note that beyond very small distances from the cathode that the translational temperatures along the plume axis are significantly lower than 300 K.

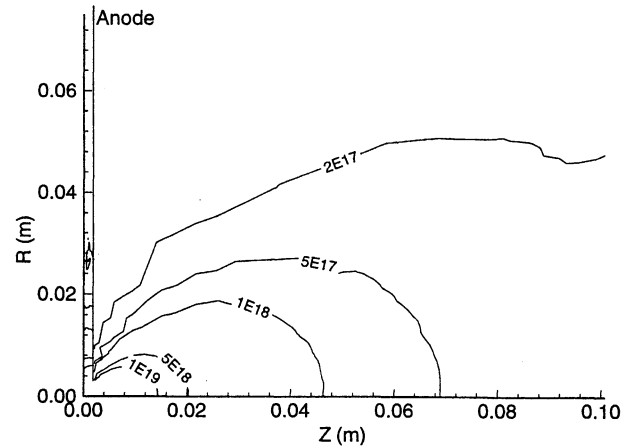


Fig. 10 Contours of number density for the plasma contactor plume.

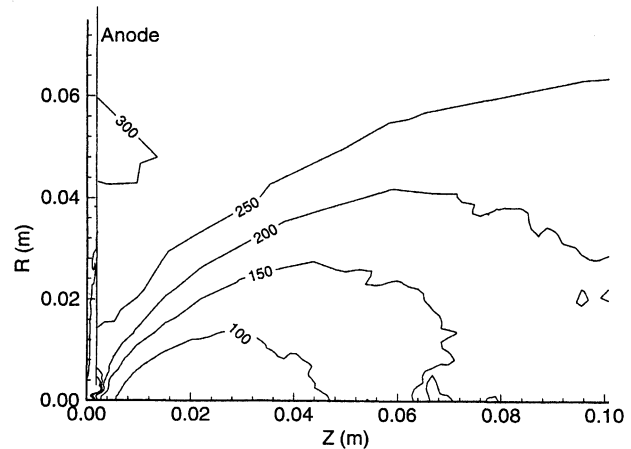


Fig. 11 Contours of translational temperature for the plasma contactor plume.

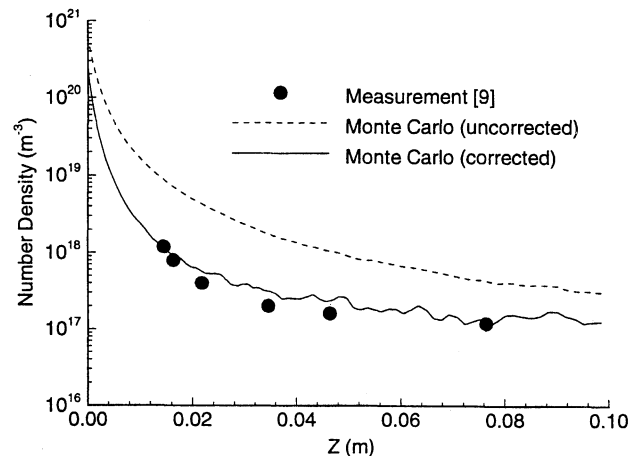


Fig. 12 Density along the axis of the plasma contactor plume.

In Fig. 12, comparison is made between the experimental measurements of Ref. 9 and the Monte Carlo computations for number density along the plume axis. Here, the origin is taken to be the plane of the anode. The data in Ref. 9 are reported as number density values, although a pressure gauge was employed. The conversion from pressure to density employed the perfect gas law and assumed the temperature to be constant at 300 K. In Fig. 12, two different sets of Monte Carlo results are shown. The first (uncorrected) is the number density actually computed by MONACO. These values are significantly higher than the experimental data. From Fig. 11, however, it is clear that the translational temperatures are not constant at 300 K for the region where the measurements were conducted. Hence, the second Monte Carlo solution (corrected) is obtained using the same procedure employed in Ref. 9. Thus, the pressure computed by MONACO based on number density and the local value of temperature is used to compute an equivalent number density using the perfect gas law and by assuming the translational temperature to be 300 K. This procedure leads to a profile that is in excellent agreement with the experimental measurements.

Hall Thruster

A laboratory scale Hall thruster has been designed and built at Stanford University for the purposes of developing diagnostic techniques.¹⁰ In Ref. 10, a laser-induced fluorescence technique was developed for measuring the velocity of neutral xenon atoms. Experimental data were reported for both cold flow (no current) and full operational conditions. The geometry of the Stanford Hall thruster is indicated in Fig. 13, in which the grid employed for the present Monte Carlo computations is shown. Xenon is injected through 32 holes with a diameter of 0.5 mm, with each hole centered at a radial distance of 4 cm from the axis. This flow passes through a small annular chamber before expanding out into the vacuum chamber. The upper and lower surfaces of this chamber are the south and north magnetic poles, respectively. The left-hand side of the chamber contains the propellant feed system and also acts as the anode. A cathode is placed above the thruster and operates with a flow rate that is 10% of that through the anode.

The cold-flow case is computed using a mass flow rate of 2.9 mg/s and assuming the flow at the injection orifice is choked. The 32 discrete orifices are modeled by a continuous annulus. All surfaces are assumed to have a temperature of 295 K. The flow from the cathode is neglected. The plume expansion is assumed to occur into perfect vacuum.

The grid shown in Fig. 13 is adapted everywhere so that cell sizes are of the order of one mean free path. Inside the first chamber, the Knudsen number (ratio of mean free path to chamber diameter) is about 0.01, placing the flow in the near

continuum regime. This flow is characterized by a relatively high collision rate requiring small computational cells. In the plume expansion, the number density falls by many orders of magnitude leading to almost collisionless flow. This allows use of much larger cells.

In Fig. 14, contours of Mach number computed inside the annular anode chamber are shown. The flow first expands rapidly to a peak Mach number of about 1.25. Then, strong viscous interaction between the fluid and the walls leads to the generation of a large boundary layer that causes deceleration of the flow. The flow then reaccelerates as it approaches the exit plane to reach the sonic condition. Beyond the exit plane the flow is supersonic.

Contours of number density in m^{-3} are shown in Fig. 15 and indicate that the plume expands rapidly away from the thruster exit. In Fig. 16, contours of computed velocity are shown. The experimental technique described in Ref. 10 provides a measurement of the velocity of neutral xenon. For the cold-flow condition, the axial velocity is measured to be 100 m/s at a point in the center of the anode chamber annulus 5 mm downstream of the exit plane. The Monte Carlo computation predicts an axial velocity of 185 m/s at this point in the flowfield. The experimental datum is surprisingly low and indicates subsonic flow. It is likely that the experimental measurement has been affected by the relatively high chamber pressure in the facility of 3×10^{-4} torr, which corresponds to a number density of 10^{19} m^{-3} at 295 K. As seen in Fig. 15, this density is reached at a small distance from the thruster exit.

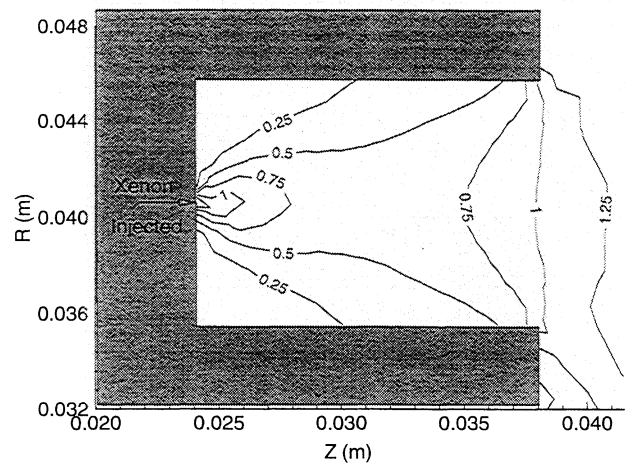


Fig. 14 Computed Mach number contours of neutral flow inside the Stanford Hall thruster for expansion to vacuum.

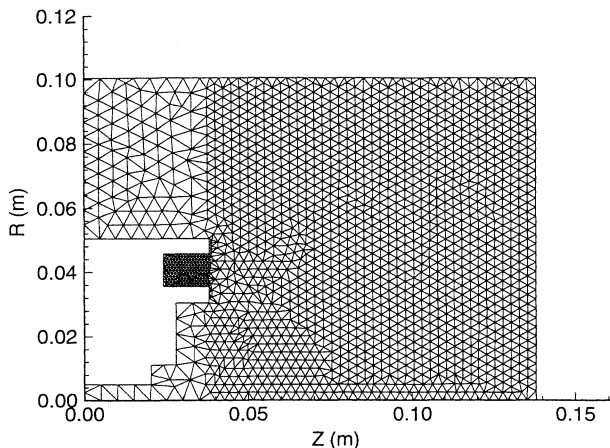


Fig. 13 Unstructured grid employed for simulation of neutral flow through the Stanford Hall thruster.

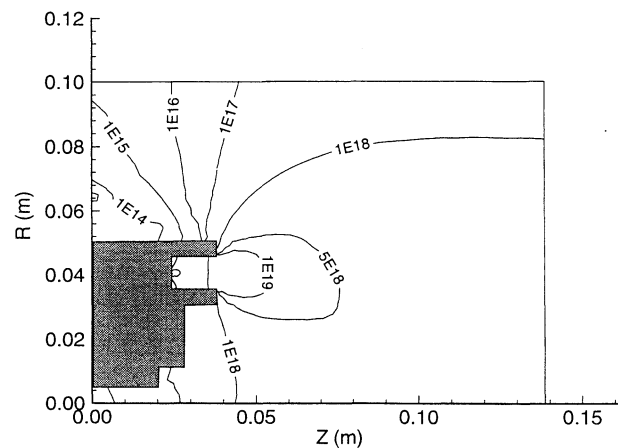


Fig. 15 Computed number density contours of neutral flow in the plume of the Stanford Hall thruster for expansion to vacuum.

A further simulation is therefore performed in which a uniform facility back pressure is imposed. The properties of the background gas are a temperature of 295 K and a number density of 10^{19} m^{-3} . The number density contours obtained under these conditions are shown in Fig. 17. Comparison with the results of Fig. 15 indicates that the area unaffected by the

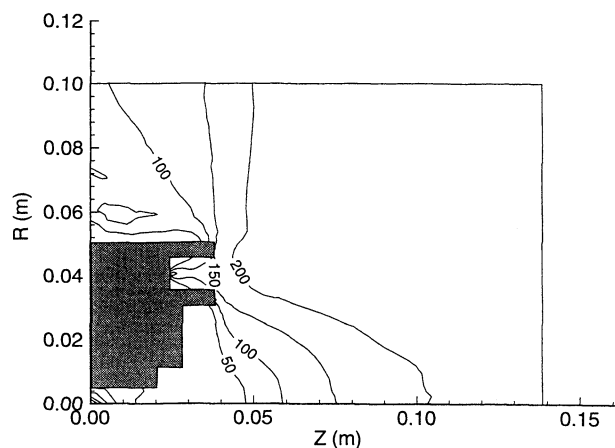


Fig. 16 Computed velocity contours of neutral flow in the plume of the Stanford Hall thruster for expansion to vacuum.

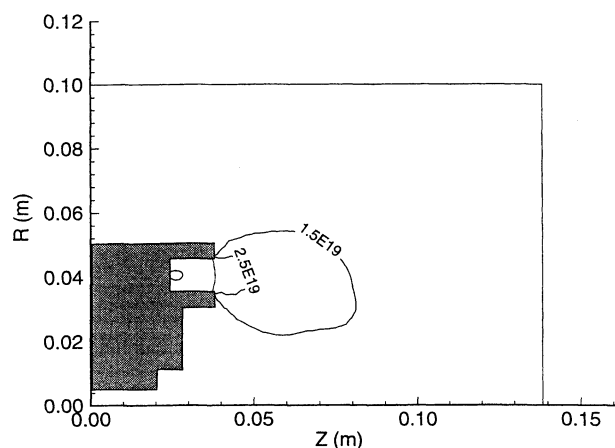


Fig. 17 Computed number density contours of neutral flow in the plume of the Stanford Hall thruster including facility back pressure.

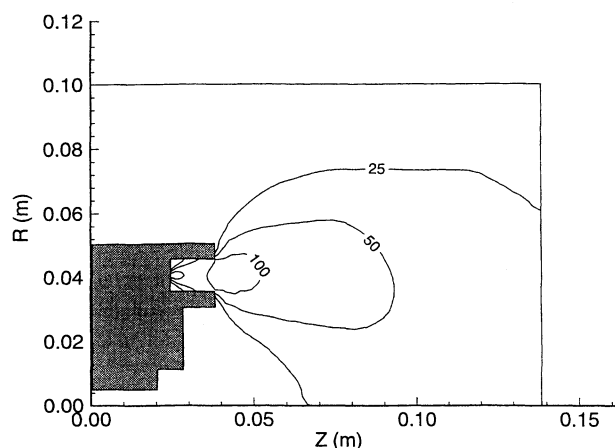


Fig. 18 Computed velocity contours of neutral flow in the plume of the Stanford Hall thruster including facility back pressure.

back pressure is very small for the conditions of the experiment. Contours of velocity shown in Fig. 18 also illustrate this point. When the facility back pressure is included, the velocity at the measurement location is computed to be 119 m/s, which is within 20% of the reported datum. This is quite acceptable given the uncertainty in the distribution of back pressure throughout the chamber. These studies suggest that the measurements reported in Ref. 10 for the Hall thruster with current flow may also be affected by facility effects. This conclusion illustrates the need for computations to be made in conjunction with such experimental investigations wherever possible.

Summary

The goal of this study was to assess the ability to accurately simulate neutral xenon flows. The motivation for the investigation is provided by the widespread use of xenon in a variety of electric propulsion devices combined with the important role played by the neutral atoms in forming charge exchange plasma. To meet this goal, numerical simulations of neutral xenon flow in three different electric propulsion configurations were performed. Specifically, flows through an ion thruster, a plasma contactor, and a Hall thruster were considered. The computations were performed using a Monte Carlo method that can simulate the relevant collision phenomena. For the UK-10 ion thruster, the Monte Carlo computations were used to assess the accuracy of a simple analytical model employed in previous studies of ion thruster plumes to approximate the distribution of neutral atoms. While reasonable agreement was obtained between the two solutions close to the plume axis, the model overpredicted density by orders of magnitude in the backflow plume region. Both sets of theoretical results were compared with number density measurements. The Monte Carlo simulations provided an excellent agreement with the experimental data. An excellent agreement of the Monte Carlo predictions with experimental data was also obtained in the plasma contactor plume. For the Hall thruster, the simulations indicated significant viscous interaction inside the annular anode chamber. Comparison of the computation for expansion into perfect vacuum with a single experimental data point for velocity indicated significant overprediction. The experimental datum was obtained in the plume flow in front of the thruster and implied subsonic flow. This would not be expected in a plume expansion and suggested some interference of the flow in the experiment. A further simulation that included the finite back pressure of the facility indicated only a small plume region outside of the thruster was unaffected by the vacuum chamber. The predicted velocity from this simulation was in a good agreement with the measured datum. In conclusion, it has been shown that the Monte Carlo computer code MONACO can provide accurate numerical simulations of neutral xenon flow in a variety of realistic electric propulsion configurations.

Acknowledgment

Funding for this research was provided by NASA Lewis Research Center through Grant NAG3-1451, Eric Pencil was the Grant Monitor.

References

- ¹Jankovsky, R., and Sankovic, J., "Performance of the FAKEL K10K Resistojet," AIAA Paper 97-3059, July 1997.
- ²Ziener, J. K., Chubbin, E. A., Choueiri, E., and Birs, D., "Performance Characterization of a High Efficiency Gas-Fed Pulsed Plasma Thruster," AIAA Paper 97-2925, July 1997.
- ³VanGilder, D. B., Font, G. I., and Boyd, I. D., "Hybrid Monte Carlo-Particle in Cell Simulation of an Ion Thruster Plume," 25th International Electric Propulsion Conf., Paper 97-182, Aug. 1997.
- ⁴Bird, G. A., *Molecular Gas Dynamics and the Direct Simulation of Gas Flows*, Oxford Univ. Press, Oxford, England, UK, 1994.
- ⁵Dietrich, S., and Boyd, I. D., "Scalar and Parallel Optimized Implementation of the Direct Simulation Monte Carlo Method," *Journal*

of *Computational Physics*, Vol. 126, 1996, pp. 328–342.

⁶Birdsall, C. K., and Langdon, A. B., *Plasma Physics Via Computer Simulation*, Adam Hilger, Bristol, England, UK, 1991.

⁷Crofton, M. W., "Measurement of Neutral Xenon Density Profile in an Ion Thruster Plume," AIAA Paper 96-2290, June 1996.

⁸Samanta Roy, R. I., Hastings, D. E., and Gatsonis, N. A., "Ion-Thruster Plume Modeling for Backflow Contamination," *Journal of*

Spacecraft and Rockets, Vol. 33, No. 4, 1996, pp. 524–534.

⁹Williams, J. D., and Wilbur, P. J., "Experimental Study of Plasma Contactor Phenomena," *Journal of Spacecraft and Rockets*, Vol. 27, No. 6, 1990, pp. 634–641.

¹⁰Cedolin, R. J., Hargus, W. A., Hanson, R. K., and Cappelli, M. A., "Laser-Induced Fluorescence Diagnostics for Xenon Hall Thrusters," AIAA Paper 96-2986, July 1996.

LIQUID ROCKET ENGINE COMBUSTION INSTABILITY

Vigor Yang and William E. Anderson, editors,
Propulsion Engineering Research Center,
Pennsylvania State University, University Park, PA

Since the invention of the V-2 rocket during World War II, combustion instabilities have been recognized as one of the most difficult problems in the development of liquid propellant rocket engines. This book is the first published in the U.S. on the subject since NASA's Liquid Rocket Combustion Instability (NASA SP-194) in 1972. Improved computational and experimental techniques, coupled with a number of experiences with full-scale engines worldwide, have offered opportunities for advancement of the state of the art. Experts cover four major subjects areas: engine

phenomenology and case studies, fundamental mechanisms of combustion instability, combustion instability analysis, and engine and component testing. Especially noteworthy is the inclusion of technical information from Russia and China, a first. Engineers and scientists in propulsion, power generation, and combustion instability will find the 20 chapters valuable as an extension of prior work and as a reference.

Contents (partial):

I. Instability Phenomenology and Case Studies

II. Fundamental Mechanisms of Combustion Instabilities

III. Combustion Instability Analysis

IV. Stability Testing Methodology

1995, 577 pp, illus, Hardback

ISBN 1-56347-183-3

AIAA Members \$64.95

List Price \$79.95

Order V-169(945)



American Institute of Aeronautics and Astronautics

Publications Customer Service, 9 Jay Gould Ct., P.O. Box 753, Waldorf, MD 20604
Fax 301/843-0159 Phone 800/682-2422 8 a.m. – 5 p.m. Eastern

CA and VA residents add applicable sales tax. For shipping and handling add \$4.75 for 1–4 books (call for rates for higher quantities). All individual orders, including U.S., Canadian, and foreign, must be prepaid by personal or company check, traveler's check, international money order, or credit card (VISA, MasterCard, American Express, or Diners Club). All checks must be made payable to AIAA in U.S. dollars, drawn on a U.S. bank. Orders from libraries, corporations, government agencies, and university and college bookstores must be accompanied by an authorized purchase order. All other bookstore orders must be prepaid. Please allow 4 weeks for delivery. Prices are subject to change without notice. Returns in sellable condition will be accepted within 30 days. Sorry, we can not accept returns of case studies, conference proceedings, sale items, or software (unless defective). Non-U.S. residents are responsible for payment of any taxes required by their government.